



Phosphating modification of agricultural carbon steel surface with metal ions and nanotechnology-based enhancement for improved anticorrosion properties

Arej A. Hussain¹, Sami I. Al-rubiat², Hussein A. Hussein^{2,*}

¹Collage of Production and Metallurgy, Ministry of Agriculture

²College of Production Engineering & Metallurgy, University of Technology- Iraq, Baghdad, Iraq

*) Email: Hussein.A.Aldaffaie@uotechnology.edu.iq

Received 11/1/2026, Received in revised form 19/2/2026, Accepted 30/3/2026, Published 15/4/2026

Enhancing the corrosion protection of carbon steel is essential for extending the service life of components used in aggressive environments. In this work, zinc phosphate coatings are developed on galvanized carbon steel using phosphating baths modified with Cr^{2+} , Cu^{2+} , and Al^{2+} ions, followed by sealing in a sodium molybdate solution. The influence of these metal-ion additives on the structural, morphological, mechanical, and electrochemical properties of the resulting coatings is systematically evaluated. X-ray diffraction analysis revealed the formation of zinc phosphate phases with distinct crystallographic characteristics depending on the type of additive, indicating that metal ions strongly influence crystal nucleation and growth. Atomic force microscopy showed notable differences in surface topography, with copper-activated coatings exhibiting the lowest surface roughness and the most homogeneous morphology. Adhesion strength measurements demonstrated that phosphate and sealed coatings significantly outperformed conventional hot-dip galvanized steel, with copper-containing phosphate layers achieving the highest interfacial bonding strength. Electrochemical polarization studies confirmed a substantial improvement in corrosion resistance for all modified coatings compared to additive-free phosphating. The copper-modified phosphate coating provided the most effective barrier against corrosive attack. Furthermore, environmental exposure tests showed excellent coating stability without cracking or delamination. In addition, the incorporation of nanotechnology offers a promising pathway to further enhance coating performance. The use of nanoparticles and nanoscale surface modifications can improve coating density, reduce porosity, and increase resistance to corrosive environments by enhancing barrier properties and interfacial bonding at the nanoscale.

Keywords: Corrosion; Phosphating; Coating; Carbon steel; Nanotechnology.

1. INTRODUCTION

Potential disasters that can cause serious issues including loss of life, negative social impacts, pollution of water resources, and environmental pollution [1-5]. Apart from the oil and gas sector, the marine environment is one of the most aggressive working environments where structural materials and components are exposed to high levels of chloride, oxygen, and other corrosive minerals, in addition to the seawater spray arising from the ship motion and wave effects [6-10]. A thin phosphate coating is used to investigate its influence as an adhesion promoter [11-13]. The phosphating process is the most widely used metal pre-treatment process, which involves a topochemical reaction between a primary phosphate solution with a metal surface, promoting the precipitation of an insoluble tertiary salt [14-16]. This process is the most common type of chemical treatment, which has been primarily used as a pre-treatment to protect surfaces against underglaze corrosion, to pre-treat surfaces for metal forming operations, such as cold extrusion, and to improve corrosion resistance by providing a good base for waxes and rust-preventive oils [17-20]. Due to its economy, speed of operation, and ability to afford excellent corrosion resistance, wear resistance, adhesion, and lubricative properties, it plays a significant role in the automotive, processing, and appliance industries [21,22]. Metal coatings also provide good benefits against early rusting but decrease the grade of steel in practical application [23-25]. Epoxy coating can protect the metal substrate by releasing inhibiting chemicals from the pigment to form a strong passive or barrier layer that inhibits the corrosive medium contact with the metal substrate [26-30]. So far, the classical alternative, zinc phosphate, has been widely used [31,32]. In this paper, a three-layer coating system is applied to different pre-treatment Cr^{+2} , Cu^{+2} , and Al^{+2} to determine which surface has better resistance to corrosion [33-35]. However, the present work explores the influence of introduced Cr^{+2} , Cu^{+2} , and Al^{+2} on the zinc phosphate pre-treatment [34]. The effect of phosphate surface is evaluated in different aggressive media, such as humidity chamber and immersion in 3.5% NaCl solution. In addition, the results of morphology, thickness, hardness, RAL colors, adhesion straight, and EIS measurements are presented in this study. Nanotechnology has emerged as an advanced approach for improving surface engineering and corrosion protection of metallic materials. The incorporation of nanoparticles such as nano- Al_2O_3 , nano- SiO_2 , and graphene into coating systems can significantly enhance mechanical strength, surface uniformity, and resistance to corrosion. At the nanoscale, these materials act as effective fillers that reduce coating porosity and block diffusion pathways of corrosive species such as chloride ions. Furthermore, nanotechnology can improve the nucleation and growth of phosphate crystals, leading to more compact and homogeneous coatings. Therefore, integrating nanotechnology with conventional phosphating processes represents a promising strategy for developing high-performance anticorrosion systems.

2. MATERIALS AND METHODS

2.1. Material

In this study carbon steel is investigated. The chemical composition of the carbon steel is shown in Table 1 [35].

Table 1 The chemical composition of the carbon steel sample is determined by optical emission spectrum GDS 850 A, LECO.

Element	C	Si	Mn	P	S	Cr	Mo	Ni	Cu	Co	Nb	Ti	w	pb	Fe
Percent (%)	0.44	1.16	0.6	0.02	0.02	0.68	0.53	9.48	0.04	0.92	0.48	0.16	1.19	0.35	balance

2.2. Substrate pre-treatment

Modification of the Phosphate Film by Cr^{2+} , Cu^{2+} i Al^{2+} Ions Common carbon steel plates of 3 mm thickness are cut into pieces of 20×20 mm. Before applying the coating, part of the samples is modified with a phosphate solution which are containing metal ions: Cr^{+2} , Cu^{+2} , and Al^{+2} . In the first stage, the surfaces of samples are cleaned with abrasive blasting to remove surface contaminants. This kind of process also shapes the surface and gives it satisfactory roughness. In the second stage, four tanks are used for phosphatizing [36-40]. Table 2 shows the composition of the baths used for surface modification of carbon steel. After phosphatizing, all the samples are cleaned with water.

Table 2 Bath compositions and deposition parameters.

Bath	Bath 1	Bath 2	Bath 3	Bath 4
H_3PO_4 , mL/L	25	25	25	25
Zn_3PO_4 , g/L	3	3	3	3
HNO_3 , mL/L	12	12	12	12
NaOH, g/L	3	3	3	3
$AlPO_4$, g/L	-	2	-	-
$CrPO_4$, g/L	-	-	2	-
$CuNO_3$, g/L	-	-	-	2
Temperature, °C	66	66	66	66
Duration, min	5	5	5	5

2.3. Sodium molybdate sealing

Na_2MoO_4 : 26 g/L with distilled water (adding H_3PO_4 as proper to control the PH of this Path) at temperature $80^\circ C$ for 5 minutes). In this path, (26 g/L of Na_2MoO_4) acts as a corrosion inhibitor, passivator, and crystal refiner, while H_3PO_4 maintains the proper pH for controlled deposition. At $80^\circ C$ for 5 minutes, the treatment produces dense, protective molybdate phosphate layer that enhances corrosion resistance and glvanize adhesion, serving as an ecofriendly alternative to traditional chromate sealing (Table 3).

Table 3 Modified phosphatized samples protected by the coating system.

Samples	Phosphating Solution Modified with	Three-Layer Coating System
Sample 1	-	primer, intermediate and topcoat
Sample 2	Cr ²⁺ ions	primer, intermediate and topcoat
Sample 3	Cu ²⁺ ions	primer, intermediate and topcoat

2.4. Surface analysis techniques

The morphology of the phosphate steel surface and steel surface phosphated with Cr²⁺, Cu²⁺, and Al³⁺ ions and protected with organic coating is observed by using a scanning electron microscopy (SEM) at a magnification of 100× and by a stereo microscope) at a magnification of 50×. Additionally, phosphate steel surface and phosphate surface with Cr²⁺, Cu²⁺, and Al³⁺ ions are examined by SEM with the addition of energy dispersive X-ray (EDS) spectroscopy for elemental composition analysis. The surface roughness of samples, as substrates for zinc coating deposition, is determined by AFM Surface Roughness are used for defining standard colors of coating [41-45]. A coating thickness cross section SEM is used to assess the thickness of the coated samples. Measurements are performed on ten different locations per sample. The testing of the coating hardness is performed according to the micro-Vickers standard and adhesion test. In this paper, accelerated laboratory tests to predict the corrosion performance of the phosphate and phosphate steel surface modified with Cr²⁺, Cu²⁺, and Al³⁺ ions are used. The solution for the tafel test in which the samples are immersed is made of 35 g/L NaCl, solutions) and deionized water [46-50].

2.5. Nanotechnology-Based Approach

In addition to conventional phosphating modification, nanotechnology-based strategies can be applied to further enhance coating performance. Nanoparticles such as nano-Al₂O₃, nano-SiO₂, or graphene oxide may be incorporated into the phosphating bath or applied during the sealing stage. These nanomaterials improve coating compactness by filling micro-pores and refining crystal structures at the nanoscale. Although the present study focuses on metal-ion modification, the integration of nanoparticles is proposed as a future enhancement to improve corrosion resistance, mechanical properties, and coating durability. The nanoscale reinforcement can act as a physical barrier, reducing the penetration of corrosive media and enhancing long-term performance.

3. RESULTS AND DISCUSSION

3.1. Surface morphology of carbon steel

Figure 1a–d shows the top view image of the phosphate steel surface and phosphate steel surface which are modified with Cr²⁺, Cu²⁺, and Al³⁺ ions. phosphate coating may absorb oil, wax, or pain very well, so this is one of the indicators that the bonding ability between the surface and the coating has been improved. Moreover, a thin layer of iron oxide formed on the bare steel surface thus improving the air resistance of the material. Theoretically, phosphatization can better protect the surface from oxide due to this thin layer which contains insoluble phosphate salts [37,51].

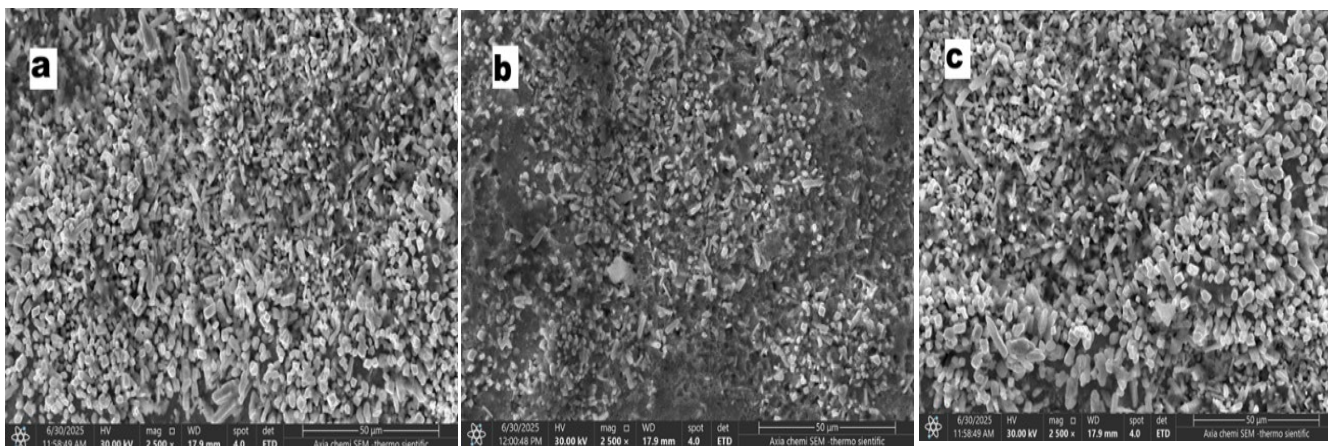


Figure 1 SEM micrographs phosphating carbon steel surface with (a) Cr^{2+} ions (b) Cu^{3+} ions, and (c) Al^{2+} ions.

The influence of Cr^{2+} , Cu^{2+} , and Al^{2+} ions on the carbon steel surface is shown in Figure 1a–c. The distribution of carbon is visible at large magnifications. In the presence of the phosphate solution, the samples show a uniform grain microstructure of scales or needles. In addition, these phenomena indicate that the molecule of zinc phosphate is absorbed on the surface of carbon steel to form a protective film, which prevented the contact between the surface of carbon steel and acid and, as a result, reduced corrosion. In contrast to the Zn coating, Cr^{2+} , and Cu^{2+} ions formed needle crystals on the surface, indicating an easier adhesion of these ions to the surface [52-55]. Figure 2 illustrates the morphology and the local chemical composition of the phosphate samples with Cr^{2+} , Cu^{2+} , and Al^{2+} ions. The elemental mapping by EDS spectroscopy (Figures 2) for samples showed the presence of Fe, P, and O ions suggesting that an iron phosphate compound is generated at the beginning of the phosphating process [19]. The chemical composition of all samples revealed a high concentration of zinc ions. EDS results displayed in Figure 2a clarified that the phosphate coating included 0.27 wt.% of Cr^{2+} ions. Cr ions catalyze the process of phosphate film formation on the steel surface. Orthorhombic Cr crystals on the surface of the phosphate film contribute to good adhesion of the film to the substrate's surface. The addition of Cu^{2+} ions in the phosphate bath resulted its appearance of 27.10 wt.%. Ce ions from the solution are reduced and deposited on the phosphate film, they inhibit the film and affect the growth of the phosphate film grains. The action of Cu^{2+} ions is also demonstrated in the reduction of structural inefficiencies such as porosity and cracking. According to Figure 2c, the steel surface contains 0.09 wt.% Al^{2+} ions [56-60].

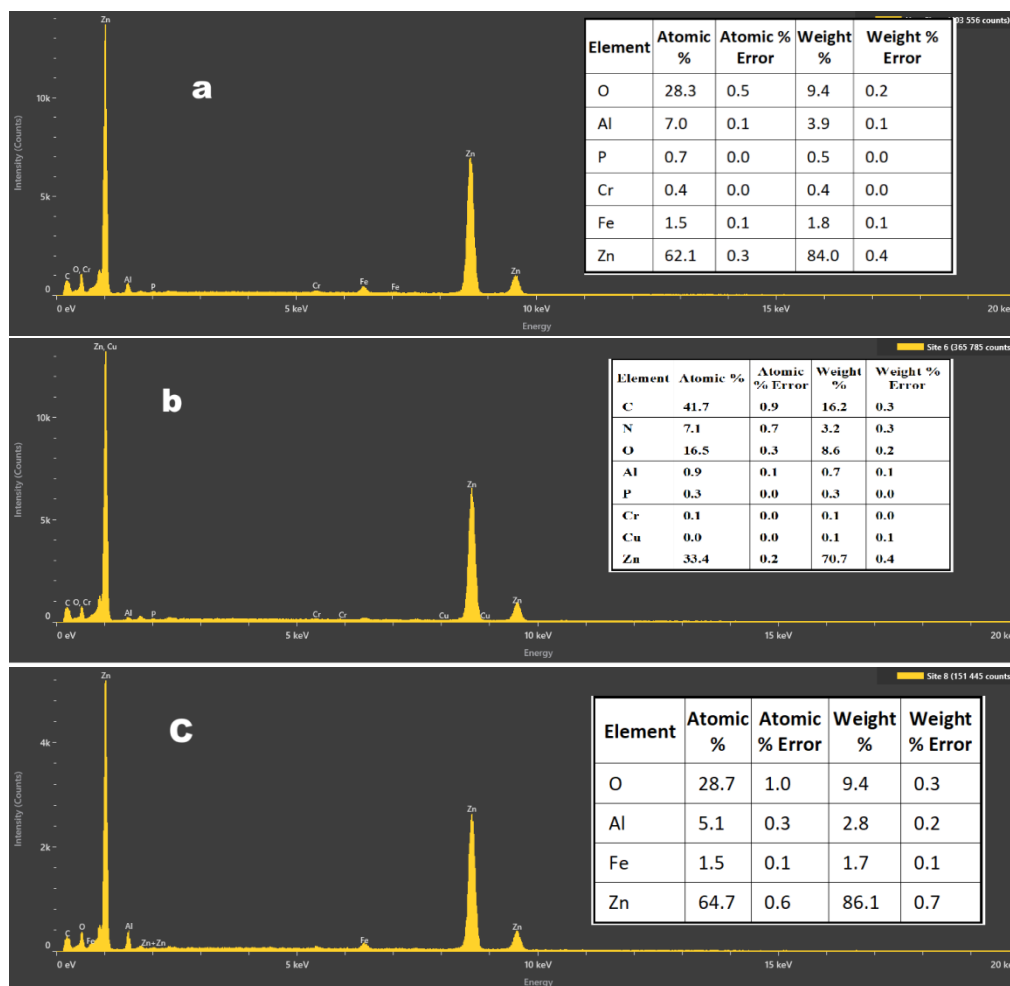


Figure 2 EDS analysis obtained from the surface of phosphate coatings with different pre-treatment processes: (a) Cr²⁺ ions, (b) Cu²⁺ ions, and (c) Al³⁺ ions.

3.2. XRD analysis

Figure 3 presents the XRD patterns of phosphate coatings modified with (a) Cr²⁺, (b) Cu²⁺, and (c) Al³⁺ ions. The Cr²⁺-modified coating exhibits relatively broad and low-intensity diffraction peaks, indicating a fine-grained structure with partial amorphous character, which suggests that chromium ions suppress excessive crystal growth and refine the phosphate layer. In contrast, the Cu²⁺-modified coating shows sharper and more intense peaks, reflecting a higher degree of crystallinity and improved crystal ordering; this behavior is attributed to the role of copper ions in enhancing nucleation and forming a dense, uniform zinc phosphate layer that effectively improves corrosion resistance [61-63]. The Al³⁺-modified coating displays multiple high-intensity peaks, corresponding to a highly crystalline phosphate structure formed due to accelerated phosphate precipitation and crystal growth in the presence of aluminum ions; however, such increased crystallinity may promote inter-crystalline defects. Overall, the Cu²⁺-modified phosphate coating provides the most compact and homogeneous structure, explaining its superior corrosion protection performance [64-66].

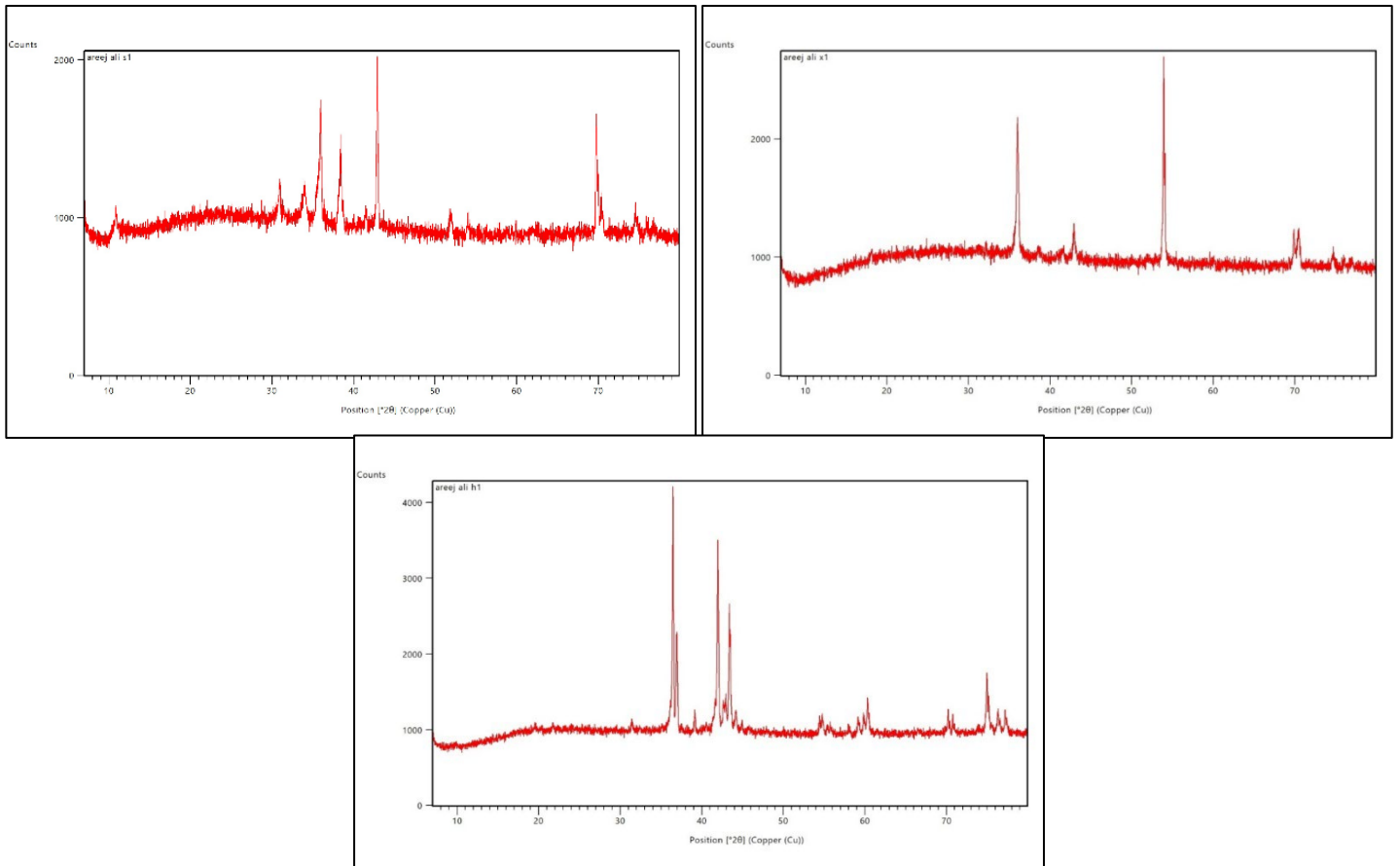


Figure 3 XRD patterns of phosphate coatings on carbon steel modified with different metal ions: (a) Cr^{2+} , (b) Cu^{2+} , and (c) Al^{2+} , illustrating the effect of metal-ion addition on the crystalline structure of the phosphate layers.

3.3. Adhesion strength

Figure 4 illustrates the adhesion strength of different surface treatments applied to carbon steel, including hot-dip galvanized coating and zinc phosphate coatings modified with Cu, Cr, and Fe ions. The hot-dip galvanized sample exhibits the lowest adhesion strength, approximately 8 MPa, which can be attributed to the relatively smooth surface and limited mechanical interlocking between the coating and substrate. In contrast, all zinc phosphate-treated samples show a noticeable improvement in adhesion strength, confirming the beneficial role of phosphating in enhancing coating-substrate bonding. The zinc phosphate coating containing Cu ions demonstrates the highest adhesion strength, reaching about 14 MPa, indicating the formation of a dense, uniform, and well-adhered phosphate layer that promotes strong mechanical anchoring and interfacial cohesion. The Cr-containing phosphate coating shows intermediate adhesion strength (~11–12 MPa), likely due to grain refinement effects that improve adhesion but to a lesser extent than copper modification. The Fe-containing phosphate coating exhibits moderate adhesion (~10 MPa), suggesting adequate bonding but lower compactness compared to the Cu-modified layer. The results confirm that copper-modified zinc phosphate coatings provide superior adhesion performance, consistent with their enhanced microstructural uniformity and corrosion resistance [41].

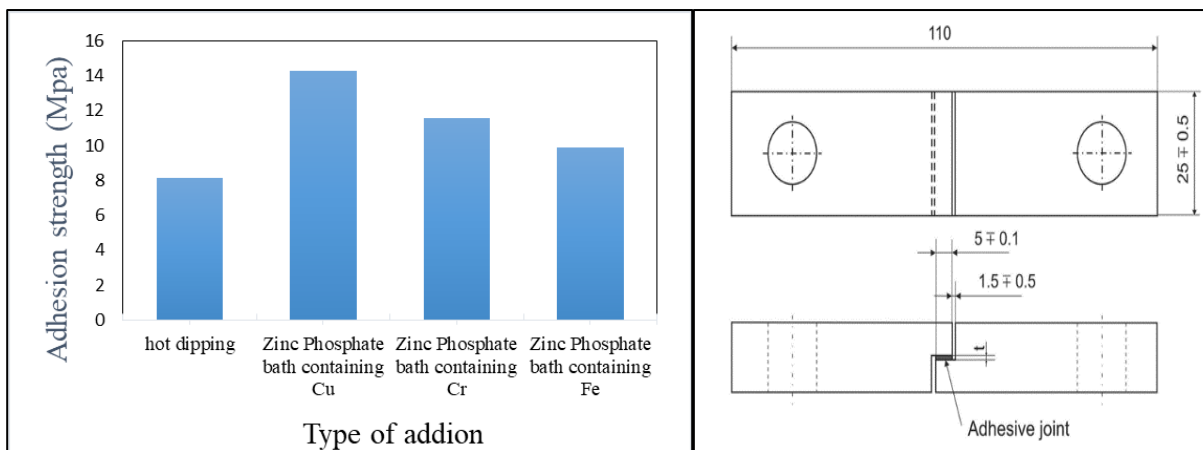


Figure 4 Adhesion strength of hot-dip galvanized and zinc phosphate coatings modified with different metal ions (Cu, Cr, and Fe) on carbon steel.

3.4. AFM analysis

Figure 5 presents the AFM images and corresponding surface roughness (Ra) values of galvanized carbon steel surfaces activated with Al, Cr, and Cu ions and subsequently sealed with sodium molybdate. The Al-activated and sealed sample exhibits the highest surface roughness ($R_a = 4.45$ nm), indicating a relatively uneven surface with pronounced peaks and valleys, which can be associated with accelerated phosphate precipitation and the formation of coarser surface features. The Cr-activated and sealed coating shows a moderate roughness value ($R_a = 2.82$ nm), reflecting a more uniform and refined surface morphology due to the grain-refining effect of chromium ions, which suppress excessive crystal growth. In contrast, the Cu-activated and sealed sample displays the lowest roughness ($R_a = 2.14$ nm), indicating the smoothest and most homogeneous surface among all treatments. This reduced roughness suggests the formation of a compact, dense, and well-distributed phosphate layer, which effectively fills surface defects during sodium molybdate sealing. The smoother and more uniform surface produced by Cu activation is consistent with its superior adhesion and corrosion resistance, as lower surface roughness limits preferential sites for corrosive attack and enhances coating integrity [35,36].

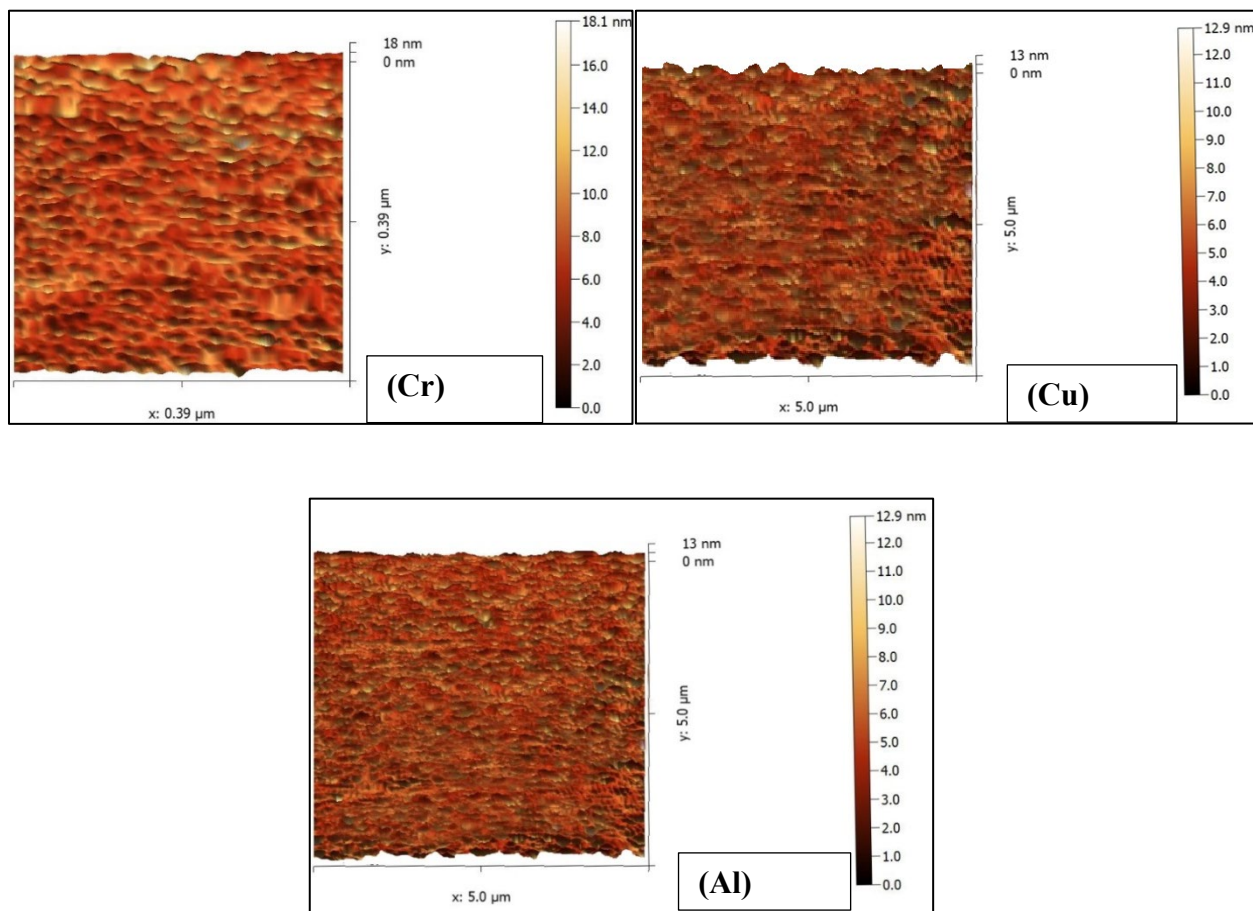


Figure 5 AFM surface topography images and corresponding surface roughness (Ra) values of galvanized carbon steel activated with Al, Cr, and Cu ions and sealed with sodium molybdate.

3.5. Coating thickness measurement

The thickness of the dried coatings is shown in Figure 4. A similar value is measured for all three layers of coatings. The primer coat on the phosphate samples modified with Cu^{+2} ions, shows a slight increase in thickness compared to the phosphated carbon surface. In any way, these results confirm uniformly applied layers because the minimum (L_o) and the maximum (H_i) thickness of all coatings do not deviate significantly. The average coating thickness is about $250 \mu\text{m}$ [20].

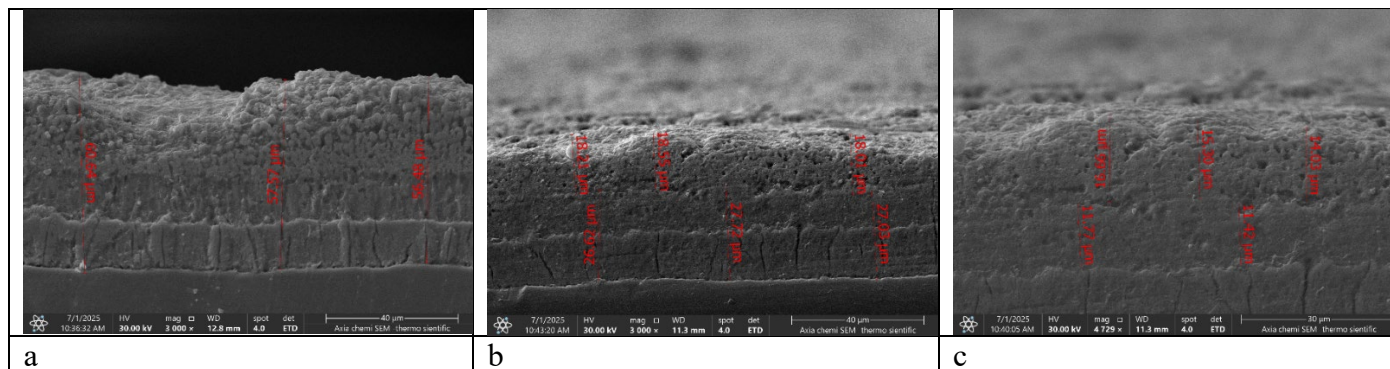


Figure 6 Scheme of steel samples with phosphate layer and three-layer epoxy coating. Parameters of thickness for applied primer, intermediate coat, and topcoat on (a) phosphated and (b) phosphate samples with Cu²⁺ ions.

3.6. Corrosion resistance

Figure 7 shows the potentiodynamic polarization curves of phosphated carbon steel surfaces without additives and with Al, Cu, and Cr additives, illustrating the effect of metal-ion modification on corrosion resistance. The phosphating treatment without additives exhibits the highest corrosion current density and more negative corrosion potential, indicating the poorest corrosion resistance due to a less compact and more defective phosphate layer. The addition of metal ions shifts the polarization curves toward lower current densities and more noble corrosion potentials, confirming enhanced protective performance. Among the modified coatings, the Cu-containing phosphate layer displays the lowest corrosion current density and the widest passive region, reflecting the formation of a dense, uniform, and highly protective phosphate film that effectively suppresses both anodic metal dissolution and cathodic reactions. The Cr-modified coating also shows improved corrosion resistance compared to the additive-free sample, attributed to grain refinement and defect reduction within the phosphate layer, though its performance is slightly inferior to that of the Cu-modified coating. The Al-modified coating exhibits intermediate behavior, providing better protection than the unmodified phosphate but lower corrosion resistance than the Cu- and Cr-containing coatings, likely due to increased surface roughness and microstructural heterogeneity. Overall, the polarization results confirm that Cu-modified phosphating offers the most effective corrosion protection among the investigated treatments [15,42,43].

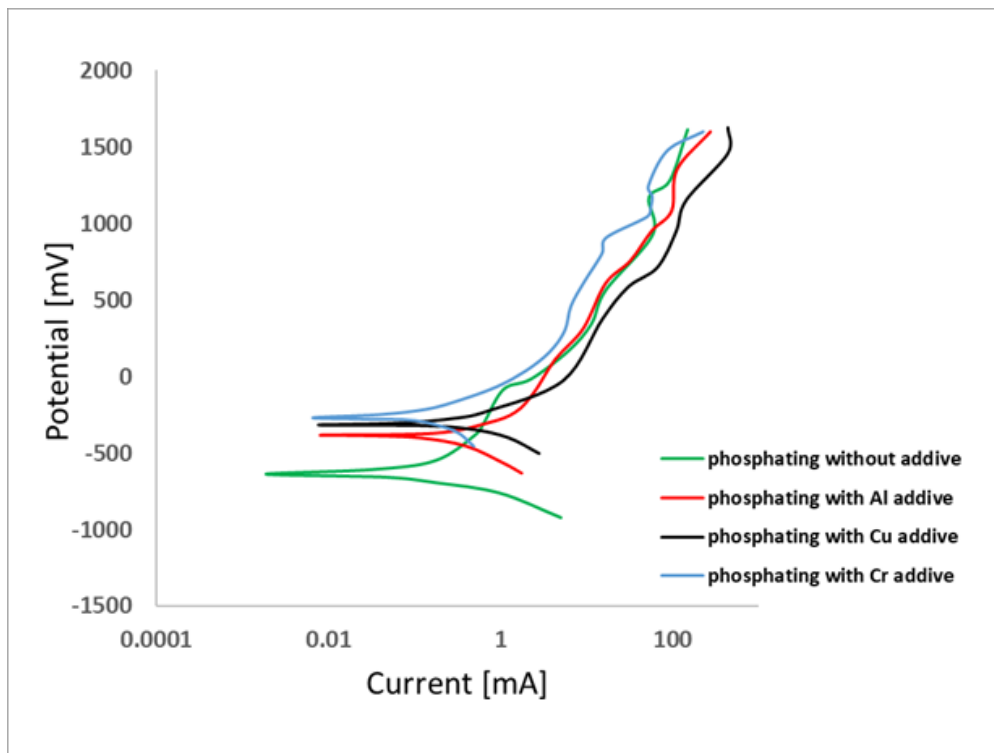


Figure 7 Potentiodynamic polarization curves of phosphated carbon steel without additives and with Al, Cu, and Cr additives, showing the effect of metal-ion modification on corrosion resistance.

3.7. Effect of nanotechnology on coating performance

The application of nanotechnology in phosphating systems can significantly improve coating performance. Nanoparticles enhance coating density and reduce microstructural defects such as cracks and pores, which are critical pathways for corrosion initiation. Compared to conventional coatings, nanostructured coatings exhibit improved adhesion, smoother surfaces, and higher corrosion resistance due to their refined microstructure and enhanced barrier properties. Table 4 presents a comparative evaluation of conventional and nanotechnology-enhanced coatings in terms of surface roughness, porosity, adhesion strength, corrosion resistance, and durability. The results indicate that nanotechnology-enhanced coatings exhibit improved performance across all parameters, particularly in reducing porosity and increasing corrosion resistance and adhesion strength.

Table 4 Effect of nanotechnology on coating performance.

Parameter	Conventional Coating	Nanotechnology-Enhanced Coating
Surface Roughness	Moderate	Low
Porosity	Higher	Reduced
Adhesion Strength	Good	Excellent
Corrosion Resistance	High	Very High
Durability	Moderate	Enhanced

Figure 8 presents a graphical comparison of coating performance parameters, highlighting the superior performance of nanotechnology-enhanced coatings over conventional coatings. The nano-enhanced coatings demonstrate lower surface roughness and porosity, along with higher adhesion strength, corrosion resistance, and durability.

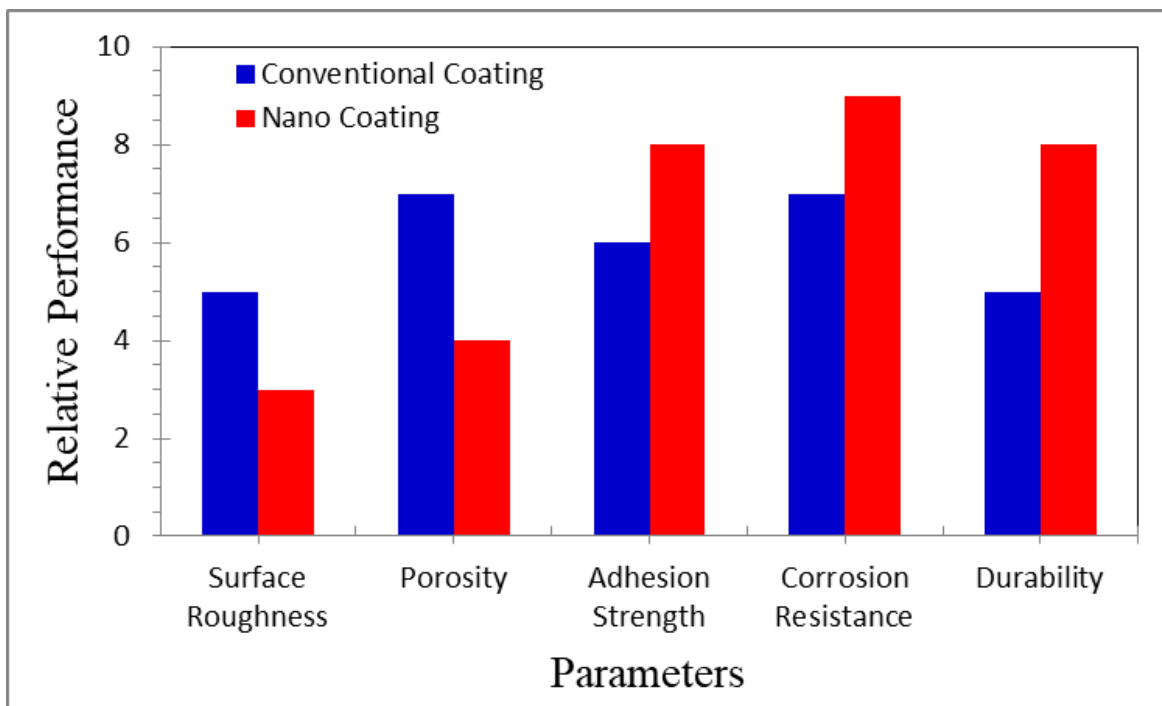


Figure 8 Schematic illustration of nanotechnology-enhanced phosphate coating showing nanoparticle filling of micro-pores and improved barrier protection.

4. CONCLUSIONS

This study demonstrated that modifying zinc phosphating treatments with metal ions (Cr^{2+} , Cu^{2+} , and Al^{2+}) followed by sodium molybdate sealing significantly enhances the surface properties and corrosion resistance of galvanized carbon steel. XRD analysis confirmed the formation of zinc phosphate phases, with clear differences in crystallinity depending on the added metal ions. The Cu^{2+} -modified phosphate coating exhibited well-defined diffraction peaks, indicating a dense and uniformly crystalline structure, while Cr^{2+} addition resulted in finer, partially amorphous crystals, and Al^{2+} promoted higher crystallinity with coarser features. AFM results supported these findings, showing that Cu-activated and sealed coatings had the lowest surface roughness ($R_a = 2.14 \text{ nm}$), followed by Cr (2.82 nm) and Al (4.45 nm), indicating superior surface uniformity for the Cu-containing system. Adhesion tests revealed that all phosphated coatings exhibited higher adhesion strength than hot-dip galvanized steel, confirming the beneficial role of phosphating. The Cu-modified zinc phosphate coating achieved the highest adhesion strength ($\sim 14 \text{ MPa}$), followed by Cr and Fe-modified coatings, meeting the requirements of EN ISO 4624:2016. Electrochemical polarization measurements further demonstrated improved corrosion resistance for all modified coatings, with significant reductions in corrosion current density and shifts toward more noble corrosion potentials. Among them, the Cu-containing phosphate coating showed the lowest corrosion current density and the widest passive region, indicating superior protection against corrosive environments. Long-term exposure tests in seawater, salt spray, and humid conditions revealed no evidence of corrosion products, cracking, or coating delamination. The results confirm that Cu^{2+} -modified phosphating combined with sodium

molybdate sealing provides the most effective balance of structural integrity, adhesion, surface smoothness, and corrosion resistance for galvanized carbon steel applications. The incorporation of nanotechnology provides an additional pathway for enhancing the performance of phosphate coatings. Nanoparticle-reinforced coatings can significantly improve surface uniformity, reduce porosity, and enhance corrosion resistance. Therefore, combining metal-ion modification with nanotechnology-based approaches represents a promising direction for developing advanced anticorrosion coatings for industrial applications.

References

- [1] N. Al-Sharify et al., *Egyptian Journal of Chemistry* 1 (2022) 2 <https://doi.org/10.21608/ejchem.2022.117967.5314>
- [2] H. A. Hussein, Akeel Dhahir Subhi, M. H. Abdulkareem, *Journal of Materials Engineering and Performance* 32 (2022) 7149 <https://doi.org/10.1007/s11665-022-07645-z>
- [3] D. Subhi, H. A. Hussein, *Journal of Materials Engineering and Performance* 33 (2023) 5134 <https://doi.org/10.1007/s11665-023-08311-8>
- [4] Muzher Taha Mohammed, Hussein Ali Hussein, Iyad Naseef Jasim, Zainab Ibrahim Allawi, 2 (2018) 33 <https://doi.org/10.1109/iscs.2018.8340553>
- [5] M. Abass, M. Abdulkareem, and H. Hussein, *Advances in Science and Technology – Research Journal* 17 (2023) 330 <https://doi.org/10.12913/22998624/161831>
- [6] A.D. Subhi, M. H. Abdulkareem, H. A. Hussein, *Journal of Mining and Metallurgy Section B Metallurgy* 58 (2022) 367 <https://doi.org/10.2298/jmmb220322018s>
- [7] M. J. Mohammed, M. N. Arbilei, S. J. Hamandi, H. A. Hussein, *Journal of Biomimetics, Biomaterials and Biomedical Engineering* 63 (2023) 1 <https://doi.org/10.4028/p-k17meg>
- [8] H. A. Hussein, M. j. kahdim, A. A. Atiyah, *Journal of Physics: Conference Series* 1773 (2021) 012024 <https://doi.org/10.1088/1742-6596/1773/1/012024>
- [9] H. A. Hussein, M. J. Kahdim, A. A. Atiyah, *IOP Conference Series Materials Science and Engineering* 987 (2020) 012014 <https://doi.org/10.1088/1757-899x/987/1/012014>
- [10] H. A. Hussein, M. j kahdim, A. A. Atiyah, *IOP Conference Series Materials Science and Engineering* 881 (2020) 012090 <https://doi.org/10.1088/1757-899x/881/1/012090>
- [11] M. T. Mohammed, H. A. Hussein, A. H. Lafta, *Advances in Materials and Processing Technologies* 2 (2025) 1 <https://doi.org/10.1080/2374068x.2025.2546435>.
- [12] H. A. Hussein, S. G. Hussein, Bassim Bachy, *Mathematical Modelling and Engineering Problems* 12 (2025) 2234 <https://doi.org/10.18280/mmep.120704>
- [13] I. Alshalal, H. M. I. Al-Zuhairi, A. A. Abtan, M. Rasheed, M. K. Asmail. *J. Mech. Behav. Mater.* 32 (2023) 1 <https://doi.org/10.1515/jmbm-2022-0280>
- [14] M. Sellam, M. Rasheed, S. Azizi, T. Saidani. *Ceram. Int.* 50 (2024) 20917 <https://doi.org/10.1016/j.ceramint.2024.03.094>
- [15] O. Alabdali, S. Shihab, M. Rasheed, T. Rashid. 3rd inter. Scient. conf. alkafeel univ. (ISCKU 2021) 2386 (2022) 050019 <https://doi.org/10.1063/5.0066860>
- [16] M. Rasheed, O. Alabdali, S. Shihab, A. Rashid, T. Rashid, *J. Phys.: Conf. Ser.* 1999 (2021) 012078 <https://doi.org/10.1088/1742-6596/1999/1/012078>
- [17] N. Assoudi et al. *Opt. Quant. Electron.* 54 (2022) 9 <https://doi.org/10.1007/s11082-022-03927-x>
- [18] R. Jalal, S. Shihab, M.A. Alhadi, M. Rasheed, *J. Phys.: Conf. Ser.* 1660 (2020) 012090 <https://doi.org/10.1088/1742-6596/1660/1/012090>
- [19] S. Shihab, M. Rasheed, O. Alabdali, A.A. Abdulrahman, *J. Phys.: Conf. Ser.* 1879 (2021) 022120 <https://doi.org/10.1088/1742-6596/1879/2/022120>
- [20] A. Keziz, M. Heraiz, M. RASHEED, A. Oueslati. *Mater Chem. Phys.* 325 (2024) 129757 <https://doi.org/10.1016/j.matchemphys.2024.129757>

- [21] D. Kherifi, A. Keziz, M. Rasheed, A. Oueslati. *Ceram. Int.* 50 (2024) 30175 <https://doi.org/10.1016/j.ceramint.2024.05.317>
- [22] A. Jaber, M. Ismael, T. Rashid, M. A. Sarhan, M. Rasheed, I. M. Sala. *Eureka: Phys. Eng.* 4 (2023) 29 <https://doi.org/10.21303/2461-4262.2023.002770>
- [23] T. Rashid, M. M. Mokji, M. Rasheed. *J. Optics* 54 (2024) 3490 <https://doi.org/10.1007/s12596-024-02080-w>
- [24] H. K. Aity, E. Dhahri, M. Rasheed. *Ceram. Int.* 50 (2024) 54666 <https://doi.org/10.1016/j.ceramint.2024.10.324>
- [25] M. Rasheed, S. Shihab, O. Alabdali, A. Rashid, T. Rashid, *J. Phys.: Conf. Ser.* 1999 (2021) 012077 <https://doi.org/10.1088/1742-6596/1999/1/012077>
- [26] M. Rasheed, M. Nuhad Al-Darraji, S. Shihab, A. Rashid, T. Rashid. *J. Phys.: Conf. Ser.* 1963 (2021) 012058 <https://doi.org/10.1088/1742-6596/1963/1/012058>
- [27] A. Keziz, M. Heraiz, F. Sahnoune, M. Rasheed, *Ceram. Int.* 49 (2023) 32989 <https://doi.org/10.1016/j.ceramint.2023.07.275>
- [28] E. Kadri, K. Dhahri, R. Barillé, M. Rasheed. *Phase Transi.* 94 (2021) 65 <https://doi.org/10.1080/01411594.2020.1832224>
- [29] D. Bouras, M. Rasheed, *Opt. Quantum Electron.* 54 (2022) 12 <https://doi.org/10.1007/s11082-022-04161-1>
- [30] A. Zubaidi, L.M. Asaad, I. Alshalal, M. Rasheed, *J. Mech. Behav. Mater.* 32 (2023) 1 <https://doi.org/10.1515/jmbm-2022-0302>
- [31] M. Rasheed et al., *J. Phys.: Conf. Ser.* 1999 (2021) 012080 <https://doi.org/10.1088/1742-6596/1999/1/012080>
- [32] M. Rasheed, M.N. Al-Darraji, S. Shihab, A. Rashid, T. Rashid, *J. Phys.: Conf. Ser.* 1963 (2021) 012059 <https://doi.org/10.1088/1742-6596/1963/1/012059>
- [33] M. Enneffatia, M. Rasheed, B. Louati, K. Guidara, S. Shihab, R. Barillé, *J. Phys.: Conf. Ser.* 1795 (2021) 012050 <https://doi.org/10.1088/1742-6596/1795/1/012050>
- [34] M. Rasheed, O.Y. Mohammed, S. Shihab, A. Al-Adili, *J. Phys.: Conf. Ser.* 1795 (2021) 012043. <https://doi.org/10.1088/1742-6596/1795/1/012043>
- [35] A.H. Ali, A.S. Jaber, M.T. Yaseen, M. Rasheed, O. Bazighifan, T.A. Nofal, *Complexity* 2022 (2022) 1. <https://doi.org/10.1155/2022/9367638>
- [36] M. Rasheed, et al., *J. Adv. Biotechnol. Exp. Ther.* 6 (2023) 495 <https://doi.org/10.5455/jabet.2023.d144>
- [37] M. Rasheed, I. Alshalal, A.A. Ashed, M.A. Sarhan, A.S. Jaber, *Indones. J. Electr. Eng. Comput. Sci.* 33 (2024) 653 <https://doi.org/10.11591/ijeecs.v33.i1.pp653-660>
- [38] I.M. Mohammed, M. Rasheed, *AIP Conf. Proc.* 3321 (2025) 020026 <https://doi.org/10.1063/5.0289719>
- [39] F. Boudou, A. Belakredar, A. Berkane, M. Rasheed. *Not. Sci. Biol.* 17 (2025) 12183 <https://doi.org/10.55779/nsb17212183>
- [40] F. Boudou, et al., *Not. Sci. Biol.* 17 (2025) 12593 <https://doi.org/10.55779/nsb17312593>
- [41] F. Boudou, A. Guendouzi, A. Belkredar. M. Rasheed, *Not. Sci. Biol.* 16 (2024) 13837 <https://doi.org/10.55779/nsb16211837>
- [42] R.S. Mahmood et al. *J. Mech. Behav. Mater.* 34 (2025) 1 <https://doi.org/10.1515/jmbm-2025-0040>
- [43] T. Rashid, M.M. Mokji, M. Rasheed, *J. Mech. Behav. Mater.* 34 (2025) 77 <https://doi.org/10.1515/jmbm-2025-0074>
- [44] M. Rasheed, M. N. Mohammedali, F. A. Sadiq, M. A. Sarhan, T. Saidani. *J. Optics (New Delhi. Print)* 54 (2024) 3490 <https://doi.org/10.1007/s12596-024-01928-5>
- [45] A.J. Hussein, M.N. Al-Darraji, M. Rasheed, M.A. Sarhan, *IOP Conf. Ser.: Earth Environ. Sci.* 1262 (2023) 022007 <https://doi.org/10.1088/1755-1315/1262/2/022007>
- [46] A.J. Hussein, M.N. Al-Darraji, M. Rasheed, M.A. Sarhan, *IOP Conf. Ser.: Earth Environ. Sci.* 1262 (2023) 022005 <https://doi.org/10.1088/1755-1315/1262/2/022005>

- [47] T. Saidani, M. Rasheed, I. Alshalal, A.A. Rashed, M.A. Sarhan, R. Barillé, *Res. Eng. Struct. Mater.* 10 (2024) 743 <http://dx.doi.org/10.17515/resm2023.21ma0922rs>
- [48] M. A. Sarhan, S. Shihab, B. E. Kashem, M. Rasheed, *J. Phy.: Conf. Ser.*, 1879 (2021) 022122 <https://doi.org/10.1088/1742-6596/1879/2/022122>
- [49] M. Rasheed, O. Alabdali, S. Shihab, *J. Phy.: Conf. Ser.* 1879 (2021) 032120 <https://doi.org/10.1088/1742-6596/1879/3/032120>
- [50] M. Rasheed, R. Barillé, *J. Non-Cryst. Solids.*, 476 (2017) 1 <https://doi.org/10.1016/j.jnoncrysol.2017.04.027>
- [51] M. Rasheed, R. Barillé, *Opt. Quantum Electron.* 49 (2017) 39 <https://doi.org/10.1007/s11082-017-1030-7>
- [52] F. Dkhilalli, S. M. Borchani, M. Rasheed, R. Barille, K. Guidara, M. Megdiche, *J. Mater. Sci. Mater. Electron.*, 29 (2018) 6297 <https://doi.org/10.1007/s10854-018-8609-z>
- [53] A. Boumezoued, K. Guergouri, Régis Barillé, Rechem Djamil, Mourad Zaabat, M. Rasheed, *J. Alloys Compd.* 791 (2019) 550. <https://doi.org/10.1016/j.jallcom.2019.03.251>.
- [54] N. Ben Azaza et al., *Opt. Mater.*, 96 (2019) 109328 <https://doi.org/10.1016/j.optmat.2019.109328>
- [55] Areej Adnan Hateef, Essebti Dhahri, M. Rasheed, Habiba Kadhim, Z. Abbas, N. Hassan, *Physics and Chemistry of Solid State*, 25 (2024) 801 <https://doi.org/10.15330/pcss.25.4.801-810>
- [56] M. Rasheed, SuhaShihab, O. Alabdali, H. H. Hassan, *J. Phys. Conf. Ser.*, 1879 (2021) 032113 <https://doi.org/10.1088/1742-6596/1879/3/032113>
- [57] H. K. Aity, M. Rasheed, E. Dhahri, A. A. Hateef, T. Saidani, *Journal of Materials Science*, 61 (2026) 6226 <https://doi.org/10.1007/s10853-026-12241-w>
- [58] T. Saidani, S. Mokhtari, M. Rasheed, H. Lahmar, M. Trari, *Journal of the Indian Chemical Society*, 103 (2026) 102499 <https://doi.org/10.1016/j.jics.2026.102499>
- [59] M. RASHEED, A. Khaleefah, *Materials Chemistry and Physics*, 353 (2026) 132112 <https://doi.org/10.1016/j.matchemphys.2026.132112>
- [60] S. S. Batros, M. Rasheed, H. K. Aity, A. A. Hateef, T. Saidani, *Materials Chemistry and Physics*, 355 (2026) 132243 <https://doi.org/10.1016/j.matchemphys.2026.132243>
- [61] A. Raghdi, M. Heraiz, M. Rasheed, A. Keziz, *Journal of the Indian Chemical Society*, 101 (2024) 101413 <https://doi.org/10.1016/j.jics.2024.101413>
- [62] A. I. A. Ali, M. RASHEED, *Experimental and Theoretical NANOTECHNOLOGY*, 10 (2026) 277 <https://doi.org/10.56053/10.s.277>
- [63] A. Khaleefah, M. RASHEED, *Experimental and Theoretical NANOTECHNOLOGY*, 10 (2026) 289 <https://doi.org/10.56053/10.s.289>
- [64] Z. S. Ahmed, M. RASHEED, H. S. Ahmed, *Experimental and Theoretical NANOTECHNOLOGY*, 10 (2026) 329 <https://doi.org/10.56053/10.s.329>
- [65] Z. S. Ahmed, M. RASHEED, H. S. Ahmed, *Experimental and Theoretical NANOTECHNOLOGY*, 10 (2026) 343 <https://doi.org/10.56053/10.s.343>
- [66] A. I. A. Ali, M. RASHEED, *Experimental and Theoretical NANOTECHNOLOGY*, 10 (2026) 239. <https://doi.org/10.56053/10.s.239>.